



OPEN

SUBJECT AREAS:
COLON CANCER
APOPTOSIS
CHEMOTHERAPYReceived
15 July 2013Accepted
24 October 2013Published
14 November 2013Correspondence and
requests for materials
should be addressed to
C.-C.C.
(chingchowchen@ntu.
edu.tw)* These authors
contributed equally to
this work.

Zebularine inhibits tumorigenesis and stemness of colorectal cancer via p53-dependent endoplasmic reticulum stress

Pei-Ming Yang^{1,2*}, Yi-Ting Lin^{1*}, Chia-Tung Shun³, Shan-Hu Lin¹, Tzu-Tang Wei¹, Shu-Hui Chuang¹, Ming-Shiang Wu⁴ & Ching-Chow Chen¹

¹Department of Pharmacology, College of Medicine, National Taiwan University, Taipei, Taiwan, ²The Ph.D. Program for Cancer Biology and Drug Discovery, College of Medical Science and Technology, Taipei Medical University, Taipei, Taiwan, ³Department of Forensic Medicine and Pathology, National Taiwan University Hospital, Taipei, Taiwan, ⁴Division of Gastroenterology, Department of Internal Medicine, National Taiwan University Hospital, Taipei, Taiwan.

Aberrant DNA hypermethylation is frequently found in tumor cells and inhibition of DNA methylation is an effective anticancer strategy. In this study, the therapeutic effect of DNA methyltransferase (DNMT) inhibitor zebularine (Zeb) on colorectal cancer (CRC) was investigated. Zeb exhibited anticancer activity in cell cultures, tumor xenografts and mouse colitis-associated CRC model. It stabilizes p53 through ribosomal protein S7 (RPS7)/MDM2 pathways and DNA damage. Zeb-induced cell death was dependent on p53. Microarray analysis revealed that genes related to endoplasmic reticulum (ER) stress and unfolded protein response (UPR) were affected by Zeb. Zeb induced p53-dependent ER stress and autophagy. Pro-survival markers of ER stress/UPR (GRP78) and autophagy (p62) were increased in tumor tissues of CRC patients, AOM/DSS-induced CRC mice and HCT116-derived colonospheres. Zeb downregulates GRP78 and p62, and upregulates a pro-apoptotic CHOP. Our results reveal a novel mechanism for the anticancer activity of Zeb.

Aberrant DNA hypermethylation is a hallmark of cancer¹. 5-aza-2'-deoxycytidine (5-Aza-CdR) and 5-azacytidine (5-Aza-CR) are potent DNA methylation inhibitors approved for treating myelodysplastic syndrome¹. Both drugs are incorporated into DNA where they bind and sequester DNA methyltransferases (DNMTs), thus prevent the maintenance of methylation status². In addition, they could elicit DNA damage response³. However, 5-Aza-CdR and 5-Aza-CR are unstable due to spontaneous aqueous hydrolysis or deamination by cytidine deaminase^{4,5}. A novel DNMT inhibitor zebularine (Zeb) is originally synthesized as a cytidine deaminase inhibitor and found to enhance the antineoplastic action of 5-Aza-CdR⁶. Zeb is very stable and preferentially targets to cancer cells without toxicity in normal cells and mice^{7,8}. However, its clinical activity is rarely investigated.

Both Zeb and 5-Aza-CR are cytidine analogues being able to incorporate into DNA and RNA. Actually, they are reported to be incorporated into RNA more than DNA^{9,10}, suggesting that RNA may be their primary target. Ribosomal RNA (rRNA) represents more than 80% of total RNA in a cell and forms the ribosomes that translate mRNAs into proteins^{11,12}. 5-Aza-CR is found to induce a rapid breakdown of liver polyribosomes¹¹. Reduced total protein synthesis by 5-Aza-CR, which is proposed to be mediated by RNA incorporation, may explain the differential effects of 5-Aza-CR and 5-Aza-CdR¹³. More specifically, RNA-dependent inhibition of ribonucleotide reductase is shown to be a major pathway for 5-Aza-CR activity¹⁴. Whether Zeb also exerts RNA-dependent effect is still unclear. Further investigation of Zeb effect may accelerate its clinical use.

The tumor suppressor p53 is maintained at low level in unstressed cells by MDM2 which ubiquitinates p53 and promotes its degradation. Both the quantity and activity of p53 are greatly increased in response to DNA damage¹⁵. p53 can induce expression of different downstream genes including *p21*, *GADD45* and *Bax* to elicit cell-cycle arrest, apoptosis and DNA repair¹⁵. In addition, p53 is stabilized by ribosomal stress. Disruption of ribosome biogenesis causes the releases of several ribosomal proteins including RPL5, RPL11, RPL23 and RPS7 from nucleolus to bind to MDM2 and prevent MDM2-mediated p53 ubiquitination and degradation¹⁶.



Endoplasmic reticulum (ER) is the site for synthesis and folding of secretory and membrane proteins. Accumulation of unfolded or misfolded proteins within ER activates unfolded protein response (UPR) through three signal pathways: protein kinase RNA-like ER kinase (PERK)/eukaryotic translation initiation factor alpha (eIF2 α), serine/threonine kinases inositol-requiring enzyme-1 (IRE1), and activating transcription factor 6 (ATF6)¹⁷. Cancer cells are often exposed to metabolic dysregulation, such as hypoxia, nutrient starvation, oxidative stress, to cause ER stress and UPR, which can provide either survival or death signals depending on the extent of ER stress¹⁸. For example, a major ER chaperone, glucose regulated protein 78 (GRP78), binds to unfolded protein to prevent further accumulation, thus promoting cell survival. However, severe or unresolved ER stress leads to apoptosis through induction of CCAAT/enhancer binding protein (C/EBP) homologous protein (CHOP) that suppresses activation of Bcl-2 and NF- κ B^{18,19}.

Colorectal cancer (CRC) is one of the most common cancers worldwide. Despite advances in surgical techniques and adjuvant therapy, there is only a modest improvement in survival of CRC patients²⁰. Thus, developing novel therapeutic strategies is still urgent. In this study, we found that Zeb exhibited *in vitro* and *in vivo* anticancer activity in cell cultures, tumor xenografts and mouse colitis-associated CRC model through induction of p53-dependent apoptosis, ER stress and autophagy. Higher expression of pro-survival ER chaperone GRP78 and autophagic marker p62 was found in tumor tissues of CRC patients and in HCT116-derived colonospheres. Zeb could downregulate GRP78 and p62, and upregulate a pro-apoptotic protein CHOP, providing a clinical intervention of Zeb in CRC.

Results

Zeb exhibited *in vitro* and *in vivo* anticancer effect. To evaluate the *in vitro* anticancer effect of Zeb, various types of human cancer cells including colon (HCT116), cervix (HeLa), lung (A549) and breast (MCF-7) were treated with Zeb. HCT116 and HeLa cells were found to be more sensitive to Zeb (Figure 1a). Consistently, Zeb-induced PARP cleavage was only seen in HeLa and HCT116 cells despite of its inhibition on DNMT1 expression in all types of cells (Supplementary Figure 1). To investigate the *in vivo* anticancer activity of Zeb, nude mice bearing HCT116 tumor xenografts were orally administered with a daily dose of 750 mg/kg for two weeks and observed for another two weeks. Both tumor volume and weight were reduced by Zeb (Figure 1b and Supplementary Figure 2). AOM/DSS-induced CRC in mice was established to further investigate the therapeutic effect of Zeb (Figure 1c, upper panel). Macroscopic observation showed that polyps were grown in the distal colon from week 8 to 11, and histological examination revealed the presence of dysplasia and adenocarcinoma (Figure 1c, lower panel and 1d). Orally administered Zeb (750 mg/kg/day) from week 8 to 11 significantly cured the polyps, and recovered the dysplasia/adenocarcinoma lesion to surface tumor necrosis (Figure 1c, lower panel and 1d). In addition, use of a lower dose of Zeb (100 mg/kg/day) also cured the polyps (data not shown). These results demonstrated that Zeb was effective for CRC treatment.

Zeb induced damages of DNA and RNA, leading to p53 activation. Zeb is a cytidine analogue being able to incorporate into DNA and RNA. After incorporation into DNA, DNMT inhibitors could induce p53 expression through DNA damage³. Zeb indeed induced DNA damage as indicated by H2AX phosphorylation (γ H2AX) and p53 expression (Figure 2a, left panel). However, the late induction of DNA damage (24 ~ 48 h) could not fully explain the rapid stabilization of p53 (6 ~ 24 h) (Figure 2a, right panel). Since Zeb is reported to be incorporated into RNA at least 7-fold greater than that of DNA⁹, RNA may be its primary target. Indeed, global RNA synthesis was inhibited by Zeb, as demonstrated by the reduced

incorporation of RNA precursor 5-bromouridine (Figure 2b, left panel). Transcription of ribosomal RNA (rRNA) constitutes up to 60% of RNA synthesis²¹. Zeb rapidly reduced the expression of 45S rRNA precursor (pre-rRNA) (Figure 2b, right panel), suggested that it might disrupt rRNA biogenesis to induce ribosomal stress and the release of ribosomal proteins. Ribosomal protein S7 (RPS7) is reported to form ternary complex with MDM2 and p53 to inhibit the E3 ligase activity of MDM2, thus leading to the stabilization of p53^{22,23}. The interaction among MDM2, p53 and RPS7 was seen, and degradation of p53 was greatly reduced in the presence of Zeb (Figure 2c, upper panels). However, RT-PCR and realtime PCR analyses demonstrated that Zeb did not alter the p53 mRNA (Figure 2c, lower panels). These results indicated that Zeb could stabilize p53 through damages of both DNA and RNA.

Zeb induced p53-dependent anticancer effect. To study the role of p53 in Zeb-induced cytotoxicity, various CRC cells with different p53 status were treated with Zeb and found that p53-mutant cells (HT29, SW480 and SW620) were more resistant to Zeb compared to p53-wildtype HCT116 and RKO cells (Figure 2d, left panel). Consistently, isogenic HCT116 p53^{-/-} cells were also more resistant to Zeb (Figure 2d, left panel). RNase protection assay showed that Zeb induced p21 mRNA expression in HCT116 wildtype but not p53^{-/-} cells (Supplementary Figure 3a). Zeb also increased p53 reporter and p21 promoter activities (Supplementary Figure 3b), and increased p21 protein expression was confirmed by western blot (Supplementary Figure 3c). Moreover, Zeb induced apoptosis in HCT116 cells, which was completely blocked in p53^{-/-} cells (Figure 2d, right panel). Therefore, the anticancer effect of Zeb was mainly dependent on p53.

Zeb induced p53-dependent ER stress, leading to cell death. Microarray analysis was performed to further address the molecular mechanisms of Zeb. Among the most significant genes induced by Zeb (> 8-fold), eight of twenty-seven genes were associated with ER stress and UPR (Supplementary Table 1). Therefore, the ER stress/UPR related genes upregulated or downregulated at least 2-fold were further categorized (Supplementary Table 2, 3 and Figure 3a). The genes that regulate ER stress associated apoptosis were induced by Zeb (31.8% of increases and 13.6% of decreases). In contrast, Zeb tended to inhibit genes that promote cell survival in response to ER stress, like chaperones/protein folding (6.9% of increases and 31% of decreases), ubiquitination/ER associated degradation (11.5% of increases and 26.9% of decreases) and unfolded protein binding/quality control (3.3% of increases and 20% of decreases) (Figure 3a). Therefore, we hypothesized that Zeb induced ER stress to promote cell death. An immediate response to protein overload in ER is the activation of PERK to phosphorylate eIF2 α and then attenuate global protein synthesis¹⁷. Zeb induced eIF2 α phosphorylation in HeLa, HCT116 and RKO but not A549 and MCF-7 cells (Figure 3b). Chemical chaperone 4-phenylbutyrate (4-PBA) was applied to examine the role of ER stress, and inhibition on Zeb-induced eIF2 α phosphorylation and cytotoxicity was seen (Figure 3c). Zeb-induced eIF2 α phosphorylation was inhibited in HCT116 p53^{-/-} cells (Figure 3d, left panel), as well as in HCT116 p53-knockdown cells (Figure 3d, right panel). Overexpression of p53 into HCT116 p53^{-/-} cells increased eIF2 α phosphorylation (Figure 3d, right panel). Therefore, Zeb induced p53-dependent ER stress to lead to cell death.

Zeb induced p53-dependent autophagic cell death. ER stress has been linked to autophagy (self-digestion) through PERK/eIF2 α and IRE1/TRAF/JNK signaling pathways²⁴. Autophagy provides an alternative energy source during starvation, thus serving as a temporary survival mechanism. However, excess autophagy can induce autophagic cell death²⁵. Autophagy can be examined by the conversion of cytosolic LC3-I to autophagosomal membrane-bound

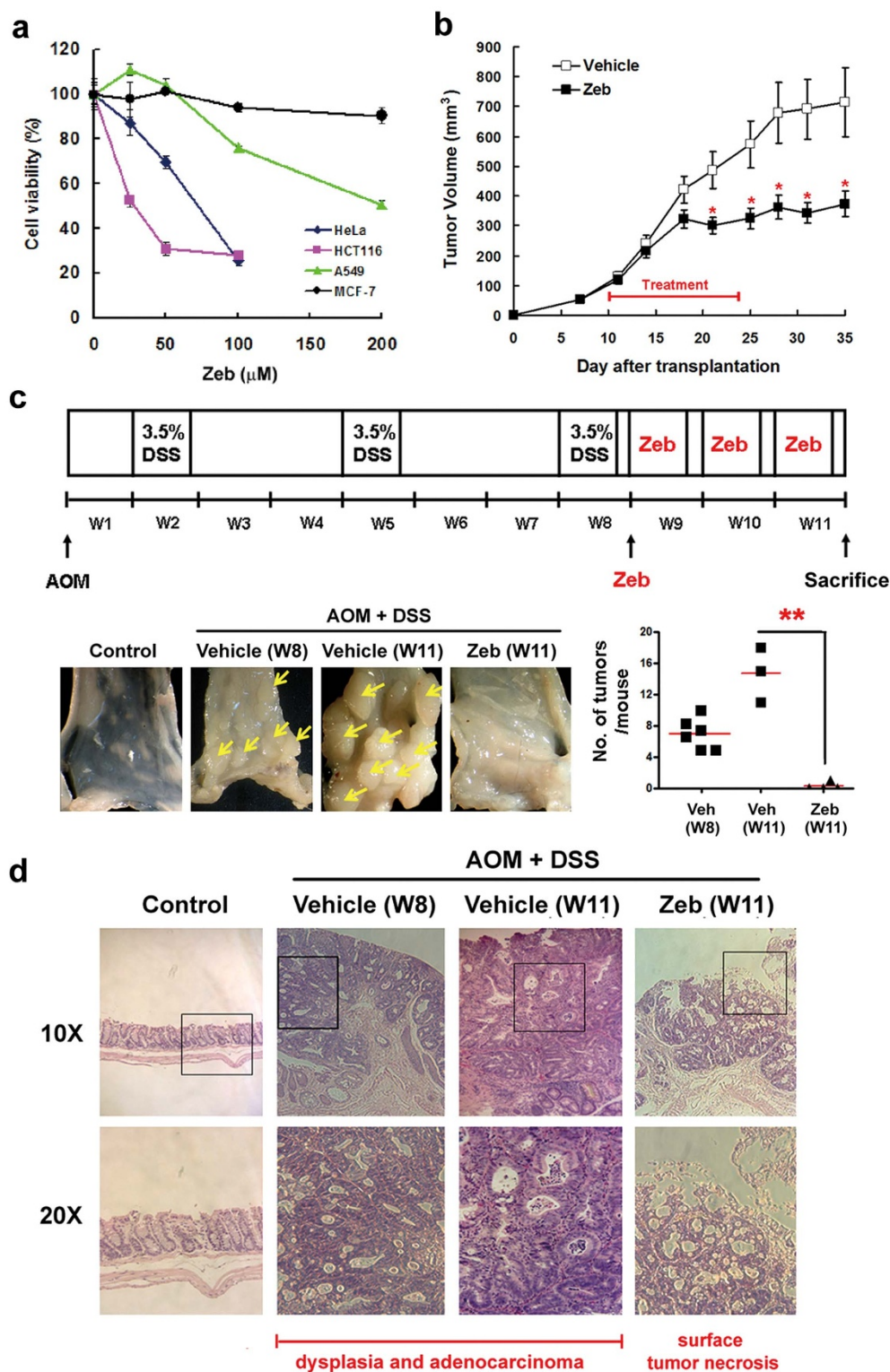


Figure 1 | Zeb exhibited *in vitro* and *in vivo* anticancer activity toward CRC. (a) HeLa, HCT116, A549, and MCF-7 cells were treated with indicated concentrations of Zeb for 3 days. The cell viability was examined by MTT assay. (b) Nude mice bearing HCT116 tumor xenografts were randomly divided into two groups and orally given with 750 mg/kg/day of Zeb ($n = 8$) or ddH₂O as vehicle ($n = 7$) for 2 weeks. After treatment, the mice were observed for another 2 weeks. The tumor volume was calculated as follows: $V = 0.52 \times (\text{the length of width})^2 \times (\text{the length of length})$. $p < 0.05$ (*) indicated the significant differences between vehicle and Zeb-treated mice. (c) Upper panel: The experimental protocol for the induction of colitis-associated colon cancer in B6 mice by AOM/DSS treatment. Lower panel: Colitis-associated colon cancer was induced in B6 mice by AOM/DSS treatment. Then, mice were orally given with 750 mg/kg/day of Zeb ($n = 4$) or ddH₂O as vehicle ($n = 3$) for three weeks. The untreated control mice were littermates of similar age. Representative photographs of murine colons were shown and the numbers of colon tumors were calculated. $p < 0.01$ (**) indicated the significant difference between vehicle and Zeb-treated mice at week 11. (d) Histologic sections (hematoxylin-eosin) showing colon samples taken from mice that received vehicle or 750 mg/kg/day of Zeb.

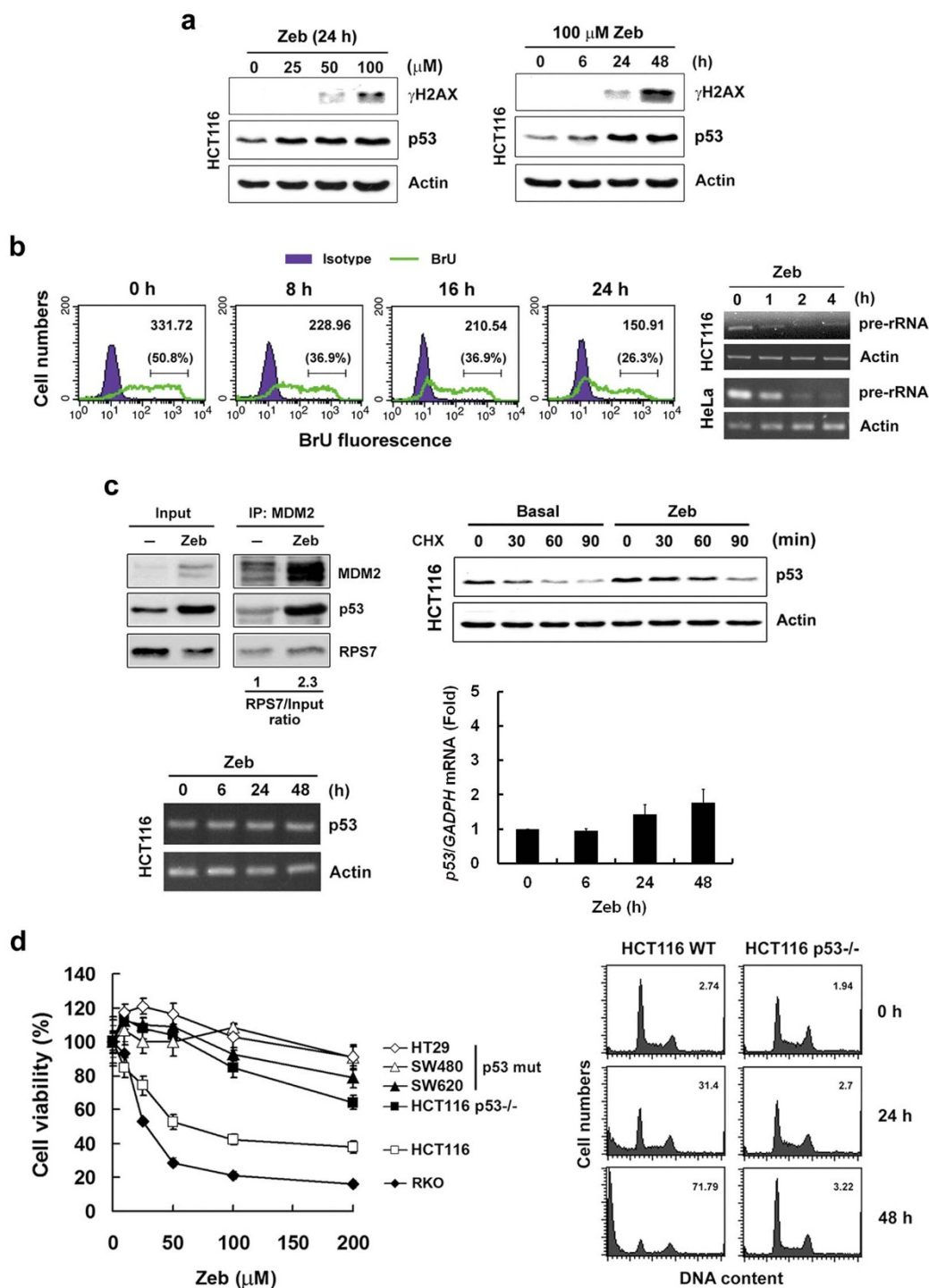


Figure 2 | Zeb stabilized p53 through DNA damage and RPS7/MDM2 pathways. (a) HCT116 cells were treated with indicated concentrations of Zeb for 24 h (left panel) or treated with 100 μM Zeb for indicated time intervals (right panel). The protein expressions of γH2AX, p53 and Actin were analyzed by western blot. (b) Left panel: HCT116 cells were treated with 100 μM Zeb for 8, 16 and 24 h and then exposed to 1 mM 5-bromouridine (BrU) 1 h before cell harvest. Cells were fixed and stained with anti-BrdU antibody. The incorporation of 5-bromouridine was analyzed by flow cytometry. The number within each histogram plot indicated the mean of BrU fluorescence and the percentage of total cells in gate. Right panel: HCT116 and HeLa cells were treated with 100 μM Zeb for indicated time intervals. The mRNA levels of 45S rRNA precursor and Actin were analyzed by RT-PCR. (c) Upper-left panel: HCT116 cells were treated with 100 μM Zeb for 16 h. Total protein lysates were immunoprecipitated with anti-MDM2 antibody. The protein expressions of MDM2, p53 and RPS7 were analyzed by western blot. Upper-right panel: HCT116 cells were treated with 100 μM Zeb for 16 h, then exposed to 10 ng/mL cycloheximide (CHX) for indicated time intervals. The protein expressions of p53 and Actin were analyzed by western blot. Lower-left and -right panels: HCT116 cells were treated with 100 μM Zeb for indicated time intervals. The mRNA levels of p53 and Actin/GAPDH were examined by RT-PCR (lower-left panel) and realtime PCR (lower-right panel). (d) Left panel: HCT116, HCT116 p53^{-/-}, RKO, HT-29, SW480 and SW620 cells were treated with indicated concentrations of Zeb for 3 days. The cell viability was examined by MTT assay. Right panel: HCT116 wildtype (WT) and p53^{-/-} cells were treated with 100 μM Zeb for indicated time intervals. The cell cycle disruption was analyzed by flow cytometry. The number within each histogram plot indicated the percentage of subG1 fraction. The images for each indicated probe in (a–c) were cropped from the same blot.

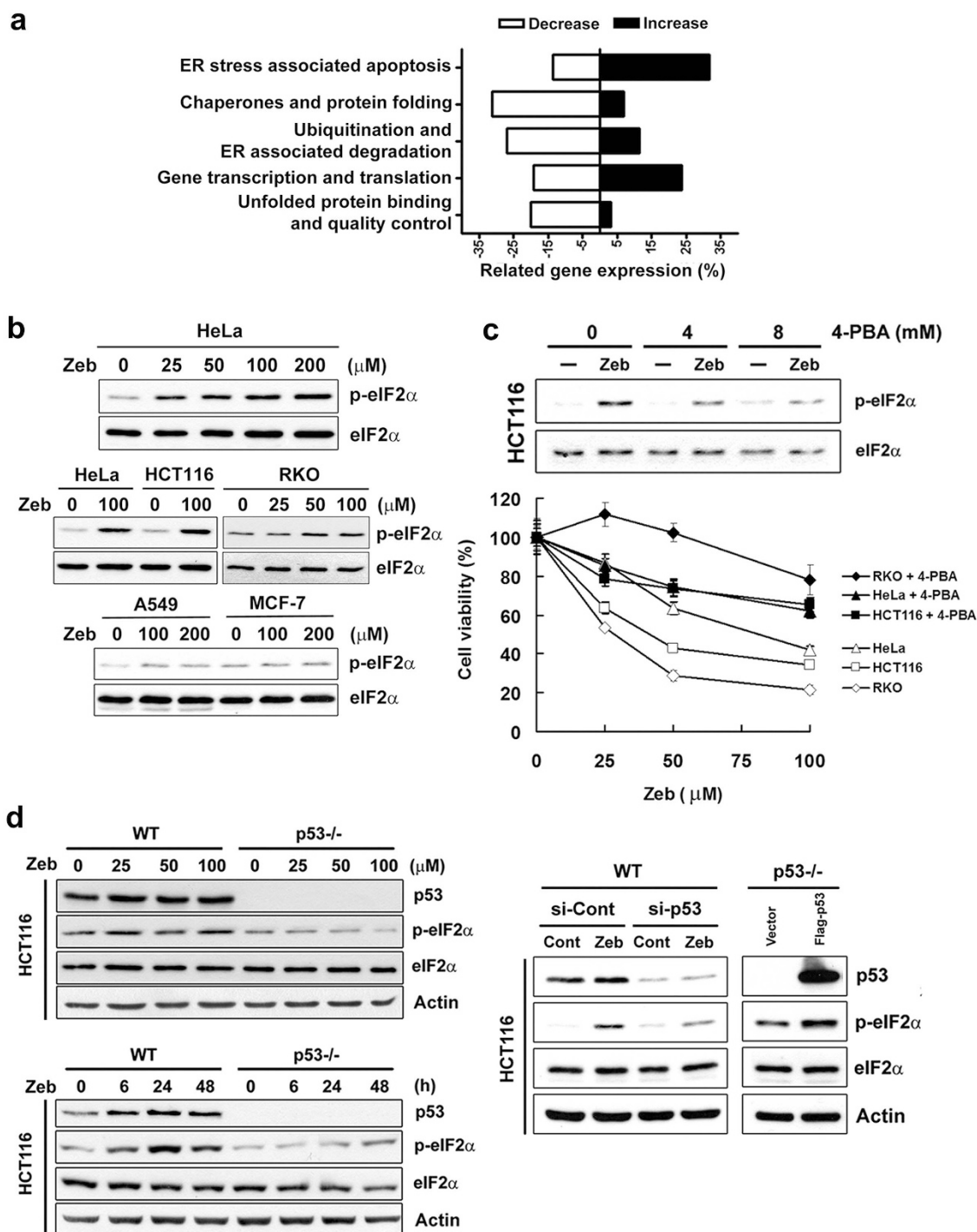


Figure 3 | Zeb induced p53-dependent ER stress leading to cell death. (a) HeLa cells were treated with 100 μM Zeb for 24 h. The global gene expression profiles were analyzed by microarray analysis. (b) HeLa (upper and middle panels), HCT116, RKO (middle panel), A549 and MCF-7 (lower panel) cells were treated with indicated concentrations of Zeb for 24 h. The protein expressions of p-eIF2 α and eIF2 α were analyzed by western blot. (c) Upper panel: HCT116 cells were pretreated with indicated concentrations of 4-PBA for 1 h and then exposed to 100 μM Zeb for 24 h. The protein expressions of p-eIF2 α and eIF2 α were analyzed by western blot. Lower panel: HeLa, HCT116 and RKO cells were pretreated with 8 mM 4-PBA for 1 h and then exposed to indicated concentrations of Zeb for 3 days. The cell viability was examined by MTT assay. (d) Left panel: HCT116 wildtype (WT) and p53 $^{-/-}$ cells were treated with indicated concentrations of Zeb for 24 h, or treated with 100 μM Zeb for indicated time intervals. The protein expressions of p53, p-eIF2 α , eIF2 α and Actin were analyzed by western blot. Right panel: HCT116 cells were transfected with 100 nM p53 siRNA for 2 days and then exposed to 100 μM Zeb for 24 h. HCT116 p53 $^{-/-}$ cells were transfected with Flag-p53 plasmid for 2 days. The protein expressions of p53, p-eIF2 α , eIF2 α and Actin were analyzed by western blot. The images for each indicated probe in (b–d) were cropped from the same blot.

LC3-II²⁶. Zeb induced LC3-II accumulation in HCT116 and RKO cells (Figure 4a, and Supplementary Figure 4), which was attenuated in HCT116 p53 $^{-/-}$ cells (Figure 4a). To analyze autophagic flux, Zeb-induced LC3-II accumulation in the presence or absence of a

vacuolar-type H⁺-ATPase inhibitor, bafilomycin A1, blocking autophagosome-lysosome fusion was analyzed. As shown in Figure 4b, the basal LC3-II was increased in response to bafilomycin A1 treatment. Zeb induced more LC3-II accumulation in



the presence of bafilomycin A1, indicating that Zeb enhanced autophagic flux. To study the role of autophagy in Zeb-induced cytotoxicity, cells were pretreated with 3-methyladenine (3-MA), a class III PI3K inhibitor that blocks autophagosome formation. Zeb-induced cytotoxicity was rescued by 3-MA in HCT116 and RKO cells (Figure 4c), as was in *Atg5*^{-/-} MEF cells, in which early stage of autophagy was suppressed (Figure 4d). These results suggest that Zeb induced p53-dependent autophagic cell death.

Clinical intervention of Zeb in CRC. ER stress can provide either survival or death signals depending on their extents¹⁸. The ER chaperone GRP78 has been reported to promote cell survival, whereas severe or unresolved ER stress leads to apoptosis through induction of CHOP¹⁸. Similarly, autophagy can also enhance cell survival or commit to autophagic death²⁴. The autophagic marker p62 is reported to promote cell survival and its elimination is found to suppress tumorigenesis²⁷. Higher eIF2 α expression and GRP78 (pro-survival)/CHOP (pro-apoptotic) ratio in tumor tissues of CRC patients compared to the adjacent normal tissues were seen (Figure 5a), suggesting that ER stress promoted tumor survival. In addition, the ratio of LC3-II/LC3-I and the p62 expression were also higher in tumor tissues (Figure 5a), indicating that autophagy also promoted cell survival in CRC tumors. These results imply the clinical benefit of Zeb for CRC patients. Indeed, Zeb inhibited the expression of GRP78 and p62, but induced CHOP in HCT116 and RKO cells (Figure 5b). To investigate whether Zeb-induced molecular events were also occurred *in vivo*, HCT116 tumor xenografts excised from mice was analyzed. Zeb induced the expression of p53 after 1 and 2 days treatment (Figure 5c, upper panel), and induced LC3-II accumulation and PARP cleavage at the end of 4 weeks experiment (Figure 5c, lower panel and Supplementary Figure 5). Zeb increased CHOP but decreased GRP78 and p62 expression in AOM/DSS-induced CRC tumors (Figure 5d). Therefore, Zeb might switch ER stress-induced pro-survival into pro-apoptotic responses, implying clinical intervention.

Zeb inhibited stemness of CRC. The existence of cancer stem cells (CSCs) in CRC is recently identified in human surgical specimens^{28–30}. CSCs are believed to mediate cancer relapse after chemotherapy³¹. The existence of CSC population in HCT116 cells was demonstrated by the formation of colonospheres (Supplementary Figure 6a), which was validated by the colorectal CSC markers CD44, CD166 and aldehyde dehydrogenase 1 (ALDH1)^{30,32} (Supplementary Figure 6b and Figure 6a). Colonospheres expressed higher levels of GRP78 and p62 (Figure 6b), and treatment with Zeb can induce phosphorylation of p53 and eIF2 α , and inhibit the ratio of GRP78/CHOP and p62 expression (Supplementary Figure 6c). Zeb reduced the ALDH-positive and CD44+/CD166+ populations in HCT116 cells (Figure 6c and Supplementary Figure 6d), indicating that Zeb might selectively target CSCs of CRC. Indeed, Zeb showed higher cytotoxicity toward colonospheres (Figure 6d).

Discussion

Zeb is a novel DNMT-inhibiting cytosine nucleoside analogue, preferentially targeting cancer cells and exhibits low toxicity toward normal cells and mice^{7,8}. Although it is more stable and oral-bioavailable compared to FDA-approved 5-Aza-CR and 5-Aza-CdR⁷, its clinical benefit has not been evaluated yet. In this study, we found that Zeb displayed anticancer activity towards CRC in cell cultures and in mice through p53-dependent apoptosis, ER stress and autophagy. CRC develops from normal epithelial cells via the aberrant crypt foci-adenoma-carcinoma sequence to metastasis. AOM/DSS-induced colitis-associated CRC in mice is found to recapitulate the nature of human colitis-associated CRC³³, thus being powerful for drug discovery. Zeb significantly eliminated the AOM/DSS-induced colon polyps with dysplasia and adenocarcinoma lesions. Examination of

CRC patients and tumor-derived stem cells showed the increased expression of pro-survival markers of ER stress/UPR (GRP78) and autophagy (p62). Zeb could downregulate GRP78 and p62, and upregulate a pro-apoptotic CHOP. These findings revealed a clinical intervention by Zeb to switch ER stress-mediated pro-survival into pro-apoptotic responses. Since CRC is still the second leading cause of cancer-related death in the world³⁴, our results provide a novel molecular insight into the anticancer mechanism of Zeb in CRC and strong rationale for its clinical trial in the future.

DNMT inhibitors could induce p53 expression through DNA demethylation or DNA damage^{33,35}. We explored an alternative pathway that DNMT inhibitors could disrupt ribosome biogenesis to cause ribosomal stress, and lead to p53 stabilization. This event occurs earlier than Zeb-induced DNA damage. The major component of ribosome is ribosomal RNA (rRNA), and pre-rRNA expression is a key step in ribosome biogenesis²¹. The accelerated synthesis of rRNA is widely found in cancers, and a number of approved therapeutic agents are reported to inhibit its synthesis³⁶. Zeb inhibited incorporation of RNA precursor, expression of pre-rRNA and induced the formation of MDM2-p53-RPS7 complex, suggesting that it might disrupt ribosome biogenesis through RNA incorporation and provides a potential therapeutic benefit.

We found that Zeb induced p53-dependent ER stress in HCT116 wildtype cells. Re-expression of p53 in HCT116 p53^{-/-} cells was sufficient to induce phosphorylation of eIF2 α . This event might depend on cell type and cellular context since Zeb did not induce ER stress in A549 cells possessing wildtype p53. The endogenous p53 in HeLa cells is known to be inactivated by HPV E6 protein³⁷, suggesting that Zeb-induced ER stress might also be independent of p53. This could explain the findings that Zeb-inhibited cell viability could not be fully rescued in HCT116 p53^{-/-} cells (Figure 2d, left panel). How p53 triggers ER stress is still unclear. Our recent study demonstrates that cytoplasmic p21 induces ER stress³⁸. However, Zeb-induced p21 only partially contributed to ER stress (Supplementary Figure 7), indicating that other p53 target genes might be involved. The eIF2 α kinase, a double-strand RNA-activated protein kinase (PKR), is also a p53 target gene and contributes to the p53-mediated apoptosis³⁹. Whether PKR is a mediator of Zeb-induced ER stress remains to be elucidated.

Severe ER stress triggers apoptosis by inducing CHOP through PERK/ATF4/eIF2 α pathway¹⁸. CHOP, also known as DNA damage-inducible protein 153 (GADD153), is a transcriptional factor that promotes apoptosis through suppression of the pro-survival Bcl-2 and upregulation of the pro-apoptotic Bim^{40,41}. Other CHOP-induced pro-apoptotic proteins include DR5, TRB3, GADD34 and CHAC1^{42–45}. We found that Zeb activated eIF2 α and induced CHOP expression and apoptosis, indicating that Zeb-induced ER stress might promote apoptosis via CHOP-dependent pathway. This is consistent with microarray analysis that Zeb induced more than 8-fold expression of TRB3, GADD34 and CHAC1 genes (Supplementary Table 1). Because CHOP has also been shown to exert anti-apoptotic function in the leukodystrophy Pelizaeus-Merzbacher disease⁴⁶, further investigation is needed to warrant its role in Zeb-induced anticancer activity.

ER stress can activate autophagy to eliminate damaged ER and abnormal protein aggregates through the lysosome pathway²⁴. Depending on the context, autophagy can enhance cell survival or commit to autophagic death²⁴. Zeb also induced autophagy in CRC cancer cells. Microarray analysis indicated that Zeb reduced genes which promote protein folding and ER-associated degradation, suggesting that Zeb may accumulate more misfolded or unfolded proteins to lead to cell death. Indeed, rescue of cell viability in *Atg5*^{-/-} MEF cells and by 3-MA demonstrated that Zeb induced autophagic cell death. How cell fate is determined after induction of autophagy is currently unclear. p62 is an autophagic marker to promote cell survival through interacting with TRAF6, a lysine 63 E3 ubiquitin ligase,

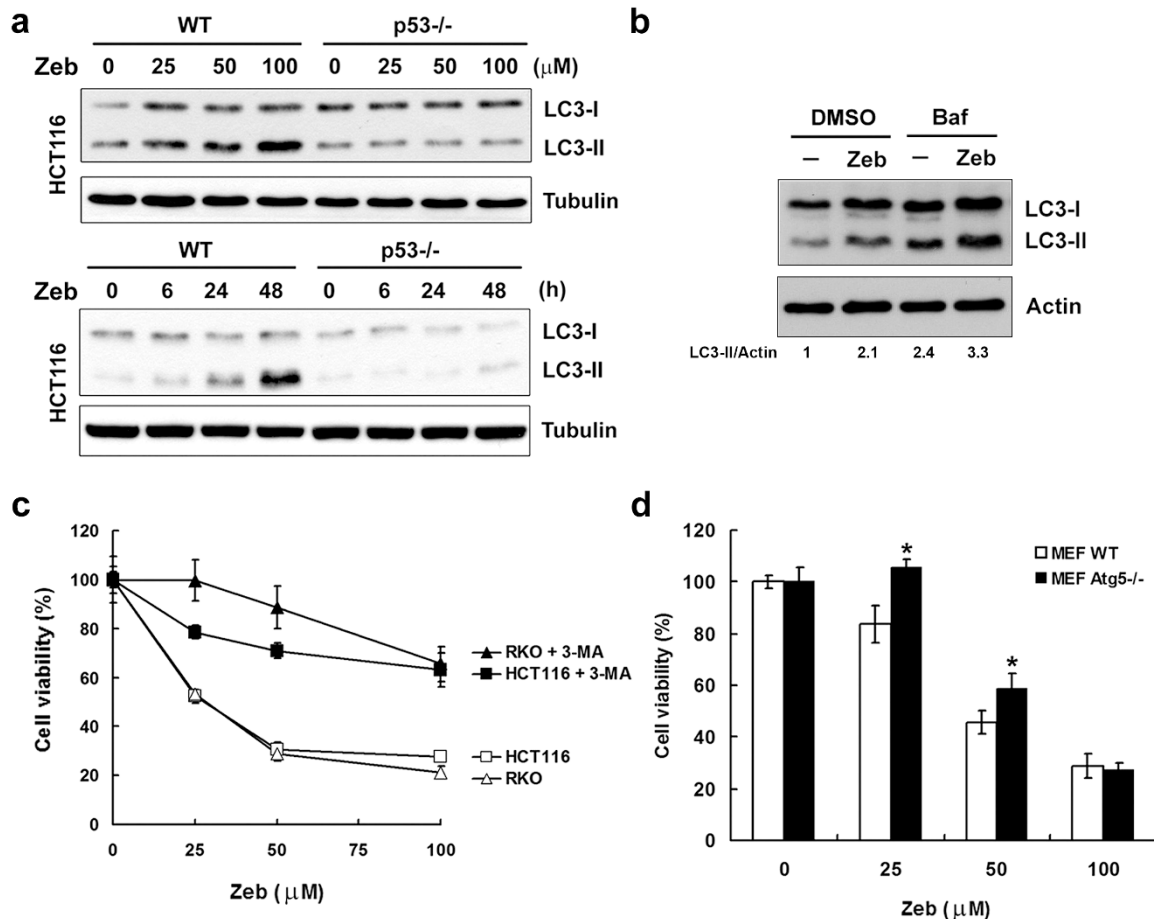


Figure 4 | Zeb induced autophagic cell death. (a) HCT116 wildtype (WT) and p53^{-/-} cells were treated with indicated concentrations of Zeb for 24 h (upper panel), or treated with 100 μM Zeb for indicated time intervals (lower panel). (b) HCT116 cells were treated with 100 μM Zeb for 24 h, then exposed to 50 nM bafilomycin A1 (Baf) for another 4 h. The protein expressions of LC3B, Tubulin and Actin in (a–b) were analyzed by western blot. (c) HCT116 and RKO cells were pretreated with 5 mM 3-MA for 1 h and then exposed to indicated concentrations of Zeb for 3 days. The cell viability was examined by MTT assay. (d) MEF wildtype (WT) and Atg5^{-/-} cells were treated with indicated concentrations of Zeb for 3 days. The cell viability was examined by MTT assay. The images for each indicated probe in (a) and (b) were cropped from the same blot.

to promote TRAF6 oligomerization and result in the activation of NF-κB⁴⁷. Thus, accumulation of p62 promotes cell survival and tumorigenesis²⁷. However, p62 binding LC3 is degraded after fusing with lysosome⁴⁸, leading to the elimination of p62 and suppression of tumorigenesis²⁷. Our results found the increase of p62 in tumor tissues of CRC patients, AOM/DSS-induced CRC mice and HCT116-derived colonospheres. Zeb could decrease the expression of p62 in cell cultures, xenografts and AOM/DSS-induced CRC mice (Figure 5b, Supplementary Figure 5 and Figure 5d), thus providing a therapeutic potential against CRC.

The existence of colorectal cancer stem cells (CSCs) in human is identified, and CRC is reported to be initiated by a rare population of crypt cells called colorectal CSCs which play an important role in metastasis and recurrence^{28–30}. Our results showed that GRP78 and p62 were correlated with the stemness of colorectal CSCs and over-expressed in tumor tissues of CRC patients and AOM/DSS-induced CRC mice. GRP78 is recognized as a putative candidate for mediating the stemness and tumorigenic properties of head and neck CSCs⁴⁹, and p62 mediates the migration and invasion of glioblastoma CSCs⁵⁰. Therefore, targeting GRP78/p62 and stemness by Zeb may provide a promising approach to treat CRC.

Previous works have focused on elucidating the molecular mechanism of Zeb as a DNA methylation inhibitor⁵¹. This study characterizes the novel action mechanism and preclinical activity of Zeb, and sheds new light on its clinical implication for CRC therapy. Future work can be conducted to put this drug or combination with

other agents into practice as a clinical therapeutic agent for CRC patients.

Methods

Materials. The antibodies specific for eIF2α (sc-11386), GRP78 (sc-1050), CHOP (sc-7351), p53 (sc-126), p21 (sc-397), MDM2 (sc-965), DNMT1 (sc-10221), PARP (sc-25780), and β-Actin (sc-161) were from Santa Cruz Biotechnology. The antibodies specific for LC3B (#2775) and phospho-Ser139-H2AX (#2577) were from Cell Signaling Technology. p62 (610832), CD44-FITC (555478) and CD166-PE (559293) antibodies were from BD Biosciences. Phospho-Ser51-eIF2α (#1090-1) antibody was from EPITOMICS. RPS7 (sc-100834) antibody was kindly provided by Dr. Edmund I-Tsuen Chen (Department of Biotechnology and Laboratory Science in Medicine, National Yang-Ming University, Taipei, Taiwan). Anti-Tubulin antibody (T6074), zebularine (Zeb; Z4775), 5-azacytidine (5-Aza-CR; A2385), 5-aza-2'-deoxycytidine (5-Aza-CdR; A3656), 3-methyladenine (3-MA; M9281), 4-phenylbutyric acid (4-PBA; P21005), bafilomycin A1 (B1793), cycloheximide (C7698) and azoxymethane (AOM; A5486) were from Sigma. Dextran sulfate sodium (DSS; 160110) was from MP Biomedicals. Recombinant human FGF-basic (bFGF; AF-100-18B) and EGF (AF-100-15) were from PeproTech. Aldefluor kit (01700) was from Stem Cell Technologies. Zebularine (NSC 309132) for animal studies was obtained from the Drug Synthesis and Chemistry Branch, Developmental Therapeutics Program, Division of Cancer Treatment and Diagnosis, National Cancer Institute. The p53-Luc expression plasmid (50125333) was from Stratagene. The p21 promoter luciferase plasmid was kindly provided by Xiao-Fan Wang (Duke University Medical Center).

Cell culture. A549, MCF-7 and HeLa cancer cells were from ATCC. RKO cells were kindly provided by Dr. Lih-Yuan Lin (Department of Life Science, National Tsing Hua University). Mouse embryonic fibroblast (MEF) wildtype and Atg5^{-/-} cells were kindly provided by Dr. Hsiao-Sheng Liu (Department of Microbiology and Immunology, College of Medicine, National Cheng-Kung University). These cells

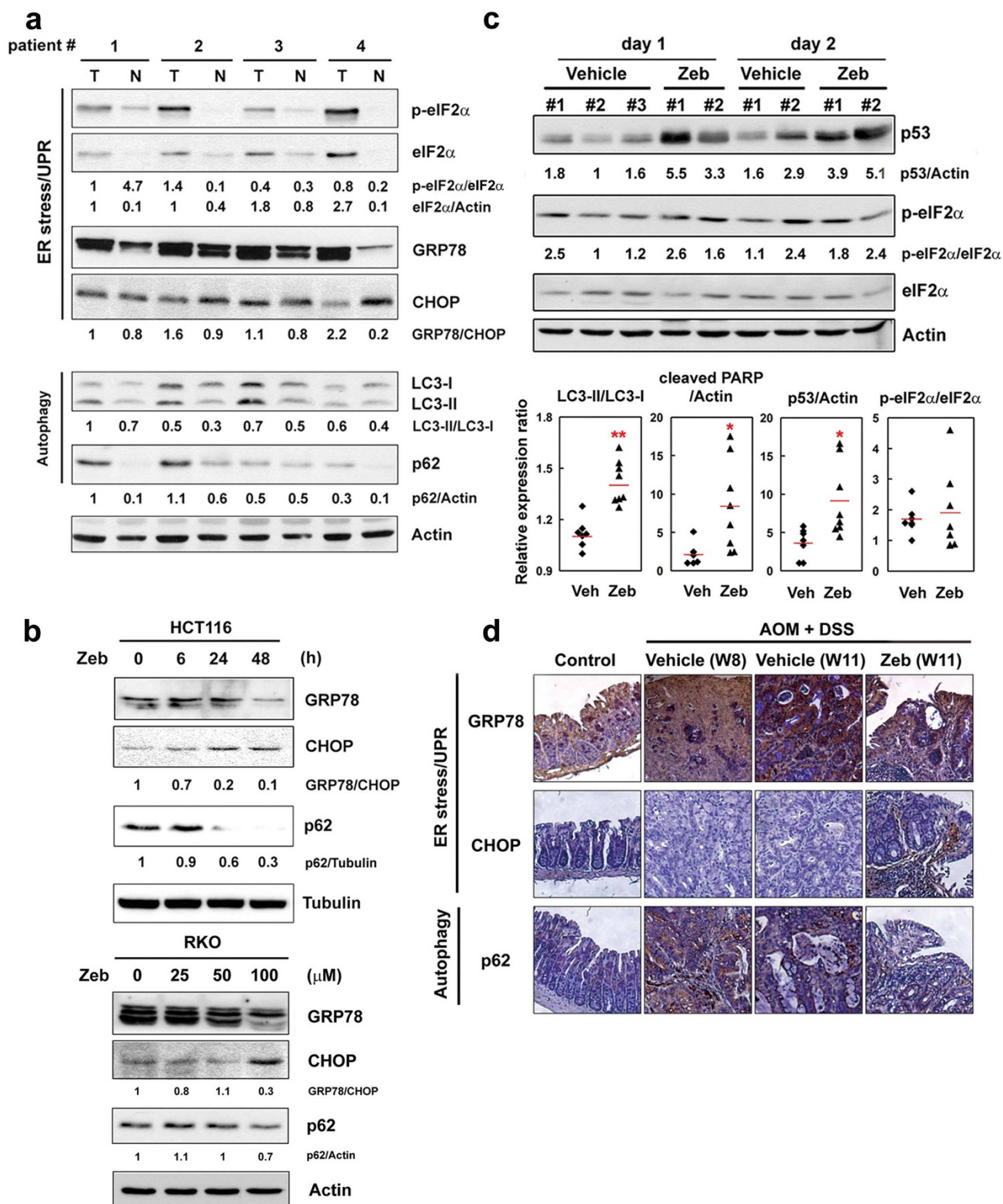


Figure 5 | Zeb promoted pro-apoptotic ER stress responses and autophagy. (a) Lysates of paired human normal and malignant colon tissues were resolved in SDS-PAGE and probed with specific antibody against p-eIF2 α , eIF2 α , GRP78, CHOP, LC3B, p62 and Actin. (b) Cells were treated with 100 μ M Zeb for indicated time intervals (HCT116), or treated with indicated concentrations of Zeb for 24 h (RKO). The protein expressions of GRP78, CHOP, p62, Tubulin and Actin were analyzed by western blot. (c) Upper panel: Nude mice bearing HCT116 tumor xenografts were orally treated with Zeb (750 mg/kg/day) for 24 and 48 h. The tumor lysates were subjected to western blot analysis. Lower panel: The tumor lysates of Figure 1b were subjected to western blot analysis. The relative expression ratio was indicated. $p < 0.05$ (*) and $p < 0.01$ (**) indicated the significant differences between vehicle and Zeb-treated mice. (d) Colon sections of Figure 1c were subjected to IHC for GRP78, CHOP and p62, and representative results were shown. The images for each indicated probe in (a–c) were cropped from the same blot.

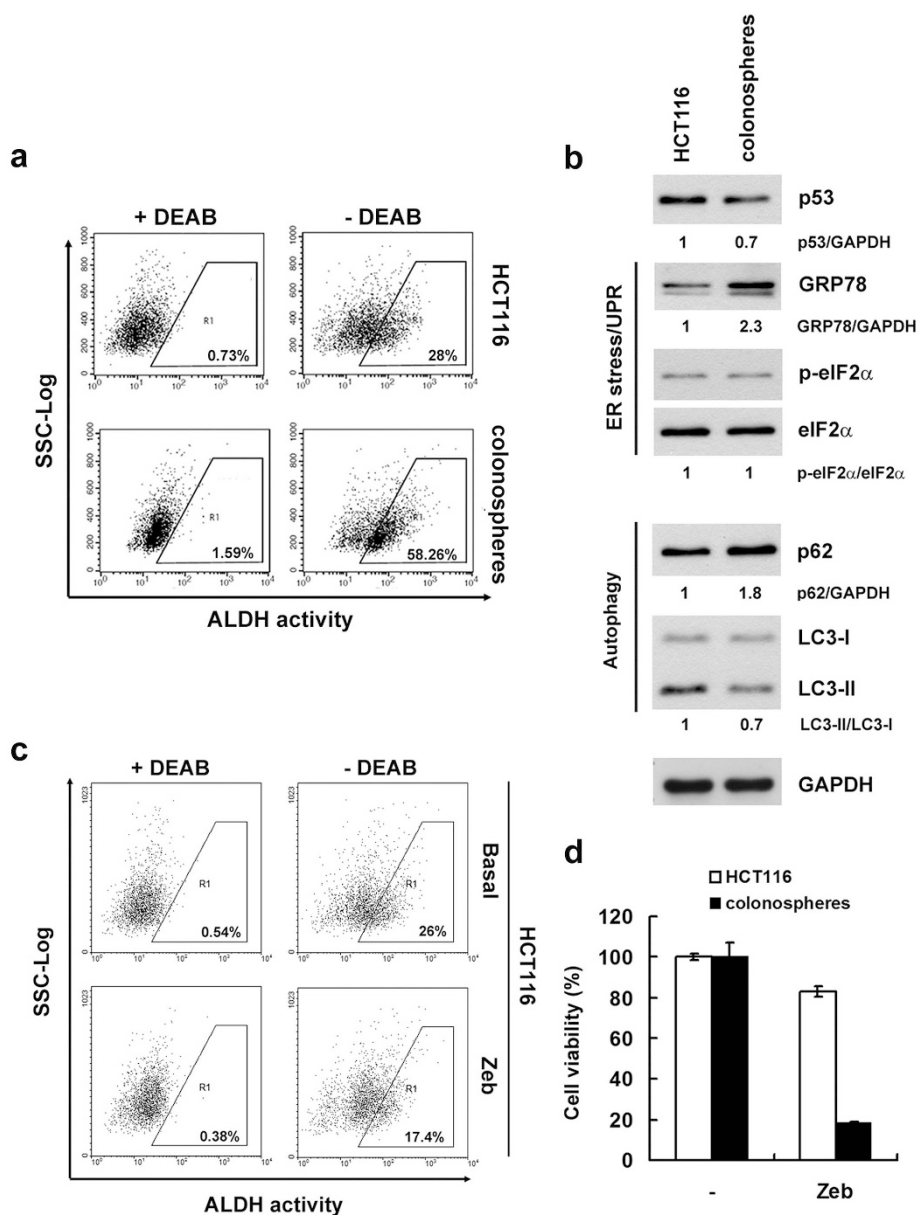


Figure 6 | Zeb inhibited stemness of CRC. (a) HCT116 cells and HCT116-derived colonospheres were dissociated and stained by Aldefluor reagent in the presence or absence of DEAB. The fluorescence was analyzed by flow cytometry. (b) Lysates of HCT116 cells and HCT116-derived colonospheres were resolved in SDS-PAGE and probed with specific antibody against p53, GRP78, p-eIF2 α , eIF2 α , p62, LC3B and GAPDH. (c) HCT116 cells were treated with 100 μ M Zeb for 24 h. Cells were stained by Aldefluor reagent in the presence or absence of DEAB. The fluorescence was analyzed by flow cytometry. (d) HCT116 cells and HCT116-derived colonospheres were dissociated and spread into 96-well plate. After treatment with 100 μ M Zeb for 48 h, cell viability was analyzed by WST-1 assay. The images for each indicated probe in (b) were cropped from the same blot.

were cultured in DMEM medium. SW480, SW620 and HT-29 cells were from ATCC. HCT116 wildtype and p53 $^{-/-}$ cells were gifts from Dr. M.W. Van Dyke (M.D. Anderson Cancer Center, Houston, TX). HCT116 p21 $^{-/-}$ cells were kindly provided by Dr. Yan-Hwa Wu Lee (Department of Biochemistry, National Yang-Ming University, Taiwan). These cells were cultured in RPMI-1640 Medium. All media were supplemented with 10% heat-inactivated FBS, 1% L-glutamine, 1% Antibiotic:Antimycotic Solution, and incubated at 37°C in a humidified incubator containing 5% CO₂.

Cell viability assay. Cell viability was measured using 3-(4,5-dimethylthiazol-2-yl)-2,5-diphenyl tetrazolium bromide (MTT) assay. Cells were plated in 96-well plates and treated with drugs. After 72 h incubation, 0.5 mg/mL MTT was added to each well for an additional 4 h. The blue MTT formazan precipitate was dissolved in 200 μ L DMSO. The absorbance at 550 nm was measured on a multiwell plate reader. For the cell viability of colonospheres, dissociated colonospheres were plated in 96-well plates and treated with Zeb for 48 h. Cell viability was examined by the cell proliferation reagent WST-1 according to the manufacturer's instructions. Cells were treated with the WST-1 reagent for 3 h, and the absorbance at 450 nm was measured.

Animal xenograft model. HCT116 cells (1×10^7) were xenografted in male Balb/c nude mice. After two weeks, animals were orally received either vehicle (ddH₂O) or Zeb (750 mg/kg/day) for two weeks and observed for another two weeks. Tumor volume was measured twice per week with calipers and calculated using the formula V (mm³) = $0.52 \times [ab^2]$, where a is the length and b is the width of the tumor. At the end of experiment, mice were sacrificed and tumors were excised. Lysates were prepared for western blot analysis. Alternatively, some tumor-bearing mice were treated with Zeb (750 mg/kg/day) for 1 and 2 days. Then, tumors were also excised and subjected for western blot analysis.

AOM/DSS-induced colitis-associated CRC in mice. Male C57BL/6 mice were intraperitoneally injected with a single dose of 12.5 mg/kg azoxymethane (AOM) on the first week and received 3.5% dextran sulfate sodium (DSS) in drinking water for 5 days at weeks 2, 5, and 8. Mice were received Zeb for three weeks after three rounds of DSS administration. All mice were sacrificed after Zeb administration and colon segments were fixed in formalin. H&E-stained colonic sections were examined for colonic aberrant crypts. All animal works were performed under protocols approved by the Institutional Animal Care and Use Committee of the College of Medicine, National Taiwan University.



Western blot analysis. After treatment, total cell lysates were prepared and subjected to SDS-PAGE. Western blot was done as described previously⁵².

Co-immunoprecipitation. Total cell lysates (500 µg) were immunoprecipitated with MDM2 antibody overnight at 4°C. Then, 20 µL protein A/G agarose was added to each sample and incubated for 2 h at 4°C. The immunoprecipitates were washed with PBS and separated using 10% SDS-PAGE. Western blot analysis was performed using antibodies specific for MDM2, p53 and RPS7.

RT-PCR and realtime PCR. Total RNA is isolated by TRIzol reagent. Reverse transcription reaction is performed using 2 µg of total RNA and reverse transcribed into cDNA using oligo dT primer, then PCR amplified using two oligonucleotide primers as following: 5'-AGACCGCGCACAGAGGAAG-3' and 5'-CTTTTGGACITCAGGTGGC-3' (p53), 5'-CCTGCTGTTCTCTCGCGCTCCGAG-3' and 5'-AACGCTGACACGCACGGCAGGAG-3' (pre-rRNA), 5'-TGACGGGGTACCCCACTGTGCCATCTA-3' and 5'-CTAGAAGCATTTGCGGGGACGATGGAGGG-3' (β-Actin). The PCR products are subjected to 1–2% agarose gel electrophoresis. Realtime PCR was performed using KAPA SYBR FAST qPCR Kit (KAPA Biosystems, KK4603) in ABI PRISM™ 7900 Sequence Detection System (Applied Biosystems). The primer sequences for p53 and GAPDH were (p53, 5'-CCCAAGCAATGGATGATTGA-3' and 5'-GGCATTCTGGGAGCTTCATCT-3') and (GAPDH, 5'-AGCCACATCGCTCAGACAC-3' and 5'-GCCCAATACGACCAAATCC-3'). All samples were read in triplicate, and values were normalized to GAPDH expression.

Transient transfection. The p53 plasmid was transiently transfected into cells with Lipofectamine 2000 Reagent. The p53 siRNA was transiently transfected into cells with Dharmafect 4 siRNA Transfection Reagent. After 24–48 h, cells were treated with Zeb for 24 h and subjected to western blot analysis.

Luciferase reporter assay. Cells were grown to 50% confluence in 12-well plates. A luciferase reporter vector that contains p53 response elements upstream of a minimal TK promoter (p53RE-Luc; 0.4 µg/well) or a luciferase reporter vector that contains p21 promoter (p21-Luc; 0.4 µg/well), and renilla luciferase reporter plasmids (p-RL-TK; 0.1 µg/well) were transiently transfected into cells with Lipofectamine 2000 Reagent. After 24 h, cells were treated with Zeb for 24 h. Cell extracts were then prepared, and luciferase activity was measured using Dual-Luciferase Reporter Assay System and normalized to renilla activity.

Cell cycle analysis. Cells were plated in 6-well plates for 24 h, then treated with complete medium containing 100 µM Zeb for 24 and 48 h. The floating and adherent cells were harvested and fixed by 70% ethanol. The cell cycle distribution was determined by flow cytometry using a PI staining buffer (5 µg/mL PI and 50 µg/mL RNase A) and analyzed on a BD FACSCalibur cytometer with CellQuest software.

5-bromouridine (BrU) incorporation assay. One hour before harvest, 5-bromouridine (BrU) was added to cell cultures to a final concentration of 1 mM. Cells were harvested and lysed with Landberg lysis buffer (PBS with 0.5% Triton X-100, 1% BSA and 0.2 µg/ml EDTA) for 15 min on ice. Then, cells were immediately fixed with 3 mL methanol at –20°C. Fixed samples were washed once with cold PBS and then incubated in 50 µL monoclonal anti-bromodeoxyuridine (BrdU) antibody, diluted 10 × in PBS/0.1% NP-40. The samples were agitated for further 60 min and then washed once with cold PBS. 50 µL polyclonal FITC-conjugated rabbit anti-mouse antibody, diluted 10 × in PBS/1%FBS, was added, and the samples were agitated for 60 min and washed once before flow cytometric analysis.

Microarray analysis. Total RNA was extracted from HeLa cells that were treated with 100 µM Zeb for 24 h. The mRNA profiles were analyzed using Affymetrix Human Genome U133 plus 2.0 GeneChip by the Microarray Core Facility of National Research Program for Genomic Medicine of National Science Council in Taiwan. GeneChips from the hybridization experiments were read by the Affymetrix GeneChip scanner 3000, and raw data were processed using GC-RMA algorithm. The raw data were also analyzed by GeneSpring GX software version 7.3.1.

Patients and specimen preparation. Specimens of tumor and adjacent normal tissue of colon were obtained from 4 patients who have been pathologically diagnosed colorectal cancer and underwent surgical resection at the National Taiwan University Hospital. Tissue specimens were ground, then sonicated in the lysis buffer (50 mM Tris-HCl, pH 7.4, 1 mM EGTA, 150 mM NaCl, 5% Triton X-100) with protease inhibitors. The samples were microcentrifuged to remove the larger debris and subjected to western analysis. All patient-derived specimens were collected and archived under protocols approved by Institutional Research Board of National Taiwan University Hospital and supported by the National Science Council of Taiwan. A full verbal explanation of the study was given to all participants. They consented to participate on a voluntary basis.

Colonsphere assay and analyses of stemness markers. HCT116 cells (2 × 10⁴ cells/mL) were cultured in serum-free DMEM/F12 medium supplemented with 1% Antibiotic:Antimycotic Solution, 1% Insulin-Transferrin-Selenium (ITS), 20 ng/mL EGF and 25 ng/mL bFGF. After 7 days, the formation of colonspheres was evaluated by light microscopy. For the analyses of CD44/CD166 expression and ALDH activity, HCT116 cells and colonspheres were dissociated by trypsinization. Freshly

dispersed cell suspension (10⁶ cells/mL) was stained in PBS/1% FBS buffer containing anti-CD44-FITC, anti-CD166-PE, or Aldefluor reagent. The fluorescence was analyzed by flow cytometry.

Statistical analysis. Means and standard deviations of samples were calculated from the numerical data generated in this study. Data were analyzed using Student's *t* test. *p* values < 0.05 were considered significant.

- Copeland, R. A., Olhava, E. J. & Scott, M. P. Targeting epigenetic enzymes for drug discovery. *Curr. Opin. Chem. Biol.* **14**, 505–510 (2010).
- Bender, C. M. *et al.* Roles of cell division and gene transcription in the methylation of CpG islands. *Mol. Cell. Biol.* **19**, 6690–6698 (1999).
- Karpf, A. R., Moore, B. C., Ririe, T. O. & Jones, D. A. Activation of the p53 DNA damage response pathway after inhibition of DNA methyltransferase by 5-aza-2'-deoxycytidine. *Mol. Pharmacol.* **59**, 751–757 (2001).
- Laliberte, J., Marquez, V. E. & Momparler, R. L. Potent inhibitors for the deamination of cytosine arabinoside and 5-aza-2'-deoxycytidine by human cytidine deaminase. *Cancer Chemother. Pharmacol.* **30**, 7–11 (1992).
- Chabner, B. A., Drake, J. C. & Johns, D. G. Deamination of 5-azacytidine by a human leukemia cell cytidine deaminase. *Biochem. Pharmacol.* **22**, 2763–2765 (1973).
- Lemaire, M., Momparler, L. F., Raynal, N. J., Bernstein, M. L. & Momparler, R. L. Inhibition of cytidine deaminase by zebularine enhances the antineoplastic action of 5-aza-2'-deoxycytidine. *Cancer Chemother. Pharmacol.* **63**, 411–416 (2009).
- Cheng, J. C. *et al.* Inhibition of DNA methylation and reactivation of silenced genes by zebularine. *J. Natl. Cancer Inst.* **95**, 399–409 (2003).
- Cheng, J. C. *et al.* Preferential response of cancer cells to zebularine. *Cancer Cell*, 151–158 (2004).
- Ben-Kasus, T., Ben-Zvi, Z., Marquez, V. E., Kelley, J. A. & Agbaria, R. Metabolic activation of zebularine, a novel DNA methylation inhibitor, in human bladder carcinoma cells. *Biochem. Pharmacol.* **70**, 121–133 (2005).
- Li, L. H., Olin, E. J., Buskirk, H. H. & Reineke, L. M. Cytotoxicity and mode of action of 5-azacytidine on L1210 leukemia. *Cancer Res.* **30**, 2760–2769 (1970).
- Cihak, A. Biological effects of 5-azacytidine in eukaryotes. *Oncology* **30**, 405–422 (1974).
- Warner, J. R. The economics of ribosome biosynthesis in yeast. *Trends Biochem. Sci.* **24**, 437–440 (1999).
- Hollenbach, P. W. *et al.* A comparison of azacitidine and decitabine activities in acute myeloid leukemia cell lines. *PLoS ONE* **5**, e9001 (2010).
- Aimiwu, J. *et al.* RNA-dependent inhibition of ribonucleotide reductase is a major pathway for 5-azacytidine activity in acute myeloid leukemia. *Blood* **119**, 5229–5238 (2012).
- Vousden, K. H. & Lu, X. Live or let die: the cell's response to p53. *Nat. Rev. Cancer* **2**, 594–604 (2002).
- Zhang, Y. & Lu, H. Signaling to p53: ribosomal proteins find their way. *Cancer Cell* **16**, 369–377 (2009).
- Shore, G. C., Papa, F. R. & Oakes, S. A. Signaling cell death from the endoplasmic reticulum stress response. *Curr. Opin. Cell Biol.* **23**, 143–149 (2011).
- Tabas, I. & Ron, D. Integrating the mechanisms of apoptosis induced by endoplasmic reticulum stress. *Nat. Cell Biol.* **13**, 184–190 (2011).
- Kim, R., Emi, M., Tanabe, K. & Murakami, S. Role of the unfolded protein response in cell death. *Apoptosis* **11**, 5–13 (2006).
- Stein, A., Atanackovic, D. & Bokemeyer, C. Current standards and new trends in the primary treatment of colorectal cancer. *Eur. J. Cancer* **47 Suppl 3**, S312–314 (2011).
- Hannan, K. M., Hannan, R. D. & Rothblum, L. I. Transcription by RNA polymerase I. *Front. Biosci.* **3**, d376–398 (1998).
- Chen, D. *et al.* Ribosomal protein S7 as a novel modulator of p53-MDM2 interaction: binding to MDM2, stabilization of p53 protein, and activation of p53 function. *Oncogene* **26**, 5029–5037 (2007).
- Zhu, Y. *et al.* Ribosomal protein S7 is both a regulator and a substrate of MDM2. *Mol. Cell* **35**, 316–326 (2009).
- Hoyer-Hansen, M. & Jaattela, M. Connecting endoplasmic reticulum stress to autophagy by unfolded protein response and calcium. *Cell Death Differ.* **14**, 1576–1582 (2007).
- Mathew, R., Karantzis-Wadsworth, V. & White, E. Role of autophagy in cancer. *Nat. Rev. Cancer* **7**, 961–967 (2007).
- Klionsky, D. J. *et al.* Guidelines for the use and interpretation of assays for monitoring autophagy. *Autophagy* **8**, 445–544 (2012).
- Mathew, R. *et al.* Autophagy suppresses tumorigenesis through elimination of p62. *Cell* **137**, 1062–1075 (2009).
- O'Brien, C. A., Pollett, A., Gallinger, S. & Dick, J. E. A human colon cancer cell capable of initiating tumour growth in immunodeficient mice. *Nature* **445**, 106–110 (2007).
- Ricci-Vitiani, L. *et al.* Identification and expansion of human colon-cancer-initiating cells. *Nature* **445**, 111–115 (2007).
- Dalerba, P. *et al.* Phenotypic characterization of human colorectal cancer stem cells. *Proc. Natl. Acad. Sci. U. S. A.* **104**, 10158–10163 (2007).
- Todaro, M., Francipane, M. G., Medema, J. P. & Stassi, G. Colon cancer stem cells: promise of targeted therapy. *Gastroenterology* **138**, 2151–2162 (2010).



32. Huang, E. H. *et al.* Aldehyde dehydrogenase 1 is a marker for normal and malignant human colonic stem cells (SC) and tracks SC overpopulation during colon tumorigenesis. *Cancer Res.* **69**, 3382–3389 (2009).
33. Tanaka, T. *et al.* A novel inflammation-related mouse colon carcinogenesis model induced by azoxymethane and dextran sodium sulfate. *Cancer Sci.* **94**, 965–973 (2003).
34. Jemal, A. *et al.* Cancer statistics, 2008. *CA. Cancer J. Clin.* **58**, 71–96 (2008).
35. Hodge, D. R. *et al.* Interleukin 6 supports the maintenance of p53 tumor suppressor gene promoter methylation. *Cancer Res.* **65**, 4673–4682 (2005).
36. Burger, K. *et al.* Chemotherapeutic drugs inhibit ribosome biogenesis at various levels. *J. Biol. Chem.* **285**, 12416–12425 (2010).
37. Kessis, T. D. *et al.* Human papillomavirus 16 E6 expression disrupts the p53-mediated cellular response to DNA damage. *Proc. Natl. Acad. Sci. U. S. A.* **90**, 3988–3992 (1993).
38. Yang, P. M. *et al.* Inhibition of autophagy enhances anticancer effects of atorvastatin in digestive malignancies. *Cancer Res.* **70**, 7699–7709 (2010).
39. Yoon, C. H., Lee, E. S., Lim, D. S. & Bae, Y. S. PKR, a p53 target gene, plays a crucial role in the tumor-suppressor function of p53. *Proc. Natl. Acad. Sci. U. S. A.* **106**, 7852–7857 (2009).
40. McCullough, K. D., Martindale, J. L., Klotz, L. O., Aw, T. Y. & Holbrook, N. J. Gadd153 sensitizes cells to endoplasmic reticulum stress by down-regulating Bcl2 and perturbing the cellular redox state. *Mol. Cell. Biol.* **21**, 1249–1259 (2001).
41. Puthalakath, H. *et al.* ER stress triggers apoptosis by activating BH3-only protein Bim. *Cell* **129**, 1337–1349 (2007).
42. Ohoka, N., Yoshii, S., Hattori, T., Onozaki, K. & Hayashi, H. TRB3, a novel ER stress-inducible gene, is induced via ATF4-CHOP pathway and is involved in cell death. *EMBO J.* **24**, 1243–1255 (2005).
43. Yamaguchi, H. & Wang, H. G. CHOP is involved in endoplasmic reticulum stress-induced apoptosis by enhancing DR5 expression in human carcinoma cells. *J. Biol. Chem.* **279**, 45495–45502 (2004).
44. Marciniak, S. J. *et al.* CHOP induces death by promoting protein synthesis and oxidation in the stressed endoplasmic reticulum. *Genes Dev.* **18**, 3066–3077 (2004).
45. Mungrue, I. N., Pagnon, J., Kohanim, O., Gargalovic, P. S. & Lusis, A. J. CHAC1/MGC4504 is a novel proapoptotic component of the unfolded protein response, downstream of the ATF4-ATF3-CHOP cascade. *J. Immunol.* **182**, 466–476 (2009).
46. Southwood, C. M., Garbern, J., Jiang, W. & Gow, A. The unfolded protein response modulates disease severity in Pelizaeus-Merzbacher disease. *Neuron* **36**, 585–596 (2002).
47. Moscat, J., Diaz-Meco, M. T. & Wooten, M. W. Signal integration and diversification through the p62 scaffold protein. *Trends Biochem. Sci.* **32**, 95–100 (2007).
48. Shvets, E., Fass, E., Scherz-Shouval, R. & Elazar, Z. The N-terminus and Phe52 residue of LC3 recruit p62/SQSTM1 into autophagosomes. *J. Cell Sci.* **121**, 2685–2695 (2008).
49. Wu, M. J. *et al.* Elimination of head and neck cancer initiating cells through targeting glucose regulated protein78 signaling. *Mol. Cancer* **9**, 283 (2010).
50. Galavotti, S. *et al.* The autophagy-associated factors DRAM1 and p62 regulate cell migration and invasion in glioblastoma stem cells. *Oncogene* **32**, 699–712 (2013).
51. Yoo, C. B., Cheng, J. C. & Jones, P. A. Zebularine: a new drug for epigenetic therapy. *Biochem. Soc. Trans.* **32**, 910–912 (2004).
52. Liu, Y. L. *et al.* Autophagy potentiates the anti-cancer effects of the histone deacetylase inhibitors in hepatocellular carcinoma. *Autophagy* **6**, 1057–1065 (2010).

Acknowledgments

This work was supported by a research grant from the National Science Council of Taiwan.

Author contributions

P.-M.Y. performed the majority of experiments and data analysis, and drafted the manuscript. Y.-T.L. performed the sphere formation assay and related experiments, and data analysis. S.-H.L. performed the related experiments in A549 cells. T.-T.W. and S.-H.C. performed mouse AOM/DSS-induced colon cancer model. C.-T.S. performed H&E stain and pathological examination. M.-S.W. provides patient specimens and pathological examination. C.-C.C. conceived and designed experiments, as well as coordinated and drafted the manuscript.

Additional information

Supplementary information accompanies this paper at <http://www.nature.com/scientificreports>

Competing financial interests: The authors declare no competing financial interests.

How to cite this article: Yang, P.-M. *et al.* Zebularine inhibits tumorigenesis and stemness of colorectal cancer via p53-dependent endoplasmic reticulum stress. *Sci. Rep.* **3**, 3219; DOI:10.1038/srep03219 (2013).



This work is licensed under a Creative Commons Attribution-NonCommercial-NoDerivs 3.0 Unported license. To view a copy of this license, visit <http://creativecommons.org/licenses/by-nc-nd/3.0>